FEMALE DRIVEN REDUCTION OF SEXUAL DIMORPHISM IN HOMININS

Thomas A. Püschel[1*+], Jorge Avaria-Llautureo[2+], Chris Venditti[2*]

1. Institute of Human Sciences, School of Anthropology and Museum Ethnography, University of Oxford, Oxford, UK.
2. School of Biological Sciences, University of Reading, Reading, UK.

* Corresponding authors.
+ These authors contributed equally to this work.

Abstract

Sexual dimorphism is a key indicator of social structure and selective pressures in primate evolution[1,2], yet its evolutionary drivers in hominins remain contentious[2,3]. Here, we combine cutting edge dimorphism estimation methods[4], with Bayesian phylogenetic comparative analyses to disentangle the sex-specific contributions and evolutionary dynamics underlying changes in body mass and canine size across over 300 hominin specimens. Our results reveal a consistent reduction in body mass dimorphism over time, driven not by male body size reduction - as is predicted by prevalent hypotheses[1,3,5,6] - but by a significant increase in female body mass. These finding challenges prevailing assumptions about the weakening of sexual selection on males and instead supports a model of positive selection on female size, likely linked to reproductive and ecological demands[3]. In contrast, canine size dimorphism is minimal throughout hominin evolution, with evidence of coordinated size reduction in both sexes, consistent with decreased reliance on canine-based competition. These patterns underscore divergent selective trajectories for different sexually dimorphic traits and highlight female-driven morphological evolution as a dominant force in hominin body size diversification. Our study provides a new framework for interpreting dimorphism in the fossil record and offers fresh insight into the evolutionary mechanisms shaping human ancestry.

Main text

The integration of novel methods for estimating dimorphism from fossil evidence with phylogenetic comparative methods provides a unique opportunity to test competing hypotheses about the evolution of sexual dimorphism in hominins. We applied a recently developed method, known as *pdpeak*[4], to data on body mass, as well as lower and upper canine size from over 300 hominins fossils to estimate dimorphism levels (Methods). The *pdPeak* method is a finite mixture model that estimates male-to-female (M/F) ratios, providing unbiased results with high accuracy, even when dimorphism within a population is minimal as in hominin's canines[4,7]. It uses Bayes theorem to evaluate the likelihood of different parameter combinations (i.e., male mean, female mean, and common within-sex variance), considering the overall shape of the sample distribution. *pdPeak* was applied for body mass ratio (BM_R), upper canine size ratio (UC_R) and lower canine size ratio (LC_R). In addition, mean estimates for female (F) and male (M) body mass and canine size were calculated using the complete posterior distribution. We also obtained female and male mean estimates for body mass (BM_F, BM_M), lower canine size (LC_F, LC_M), and upper canine size (UC_F, UC_M).

As sexual dimorphism in fossil samples can be estimated using multiple methods, we also assessed our results using two additional metrics representatives of the most reliable grouping and variance-based dimorphism methods to date[8]. We computed the Mean Method Ratio (*MMR*), and a variance-based method, which is the Standard Deviation of Logged Data (*sdlog*). Our comparative results are qualitatively identical regardless of the dimorphism metric used, demonstrating the robustness of our findings (see Supplementary Information).

Our results reveal that many members of genus *Homo* showed lower levels of BM_R ($BM_R < 1.15$ in *H. sapiens*, *H. heidelbergensis*, and *H. neanderthalensis*) as compared to other hominin such as *Paranthropus robustus* ($BM_R = 1.19$), *P. boisei* ($BM_R = 1.32$), *Australopithecus africanus* ($BM_R = 1.32$, and *Au. Afarensis* ($BM_R = 1.62$). These earlier species show BM_R levels comparable to those observed in genera such as *Alouatta, Lophocebus* or *Cercopithecus*. *Au. afarensis* is the most sexually dimorphic hominin in our sample, displaying levels of dimorphism comparable to those found in species characterized by high male intra-sexual competition and polygynous mating systems, such as *Theropithecus gelada* and *Papio kindae*. Nevertheless, it is worth noting that some members of the genus *Homo*, such as *H. habilis*, also exhibited higher levels of dimorphism ($BM_R = 1.37$). At the other end of the spectrum are *H. sapiens*, *H. heidelbergensis*, and *H. neanderthalensis* (Figure 1) - whose BM_R levels are comparable to those of some hylobatids, a group typically characterised as monogamous. For both UC_R and LC_R, all hominin species exhibit values that are markedly lower than those observed in other hominines like African apes (Figure 1), and far below those of highly dimorphic anthropoids such as mandrills *(Mandrillus)* or baboons (*Papio*). In fact, most hominin canine dimorphism levels more closely resemble those of hylobatids as compared to any other ape species.

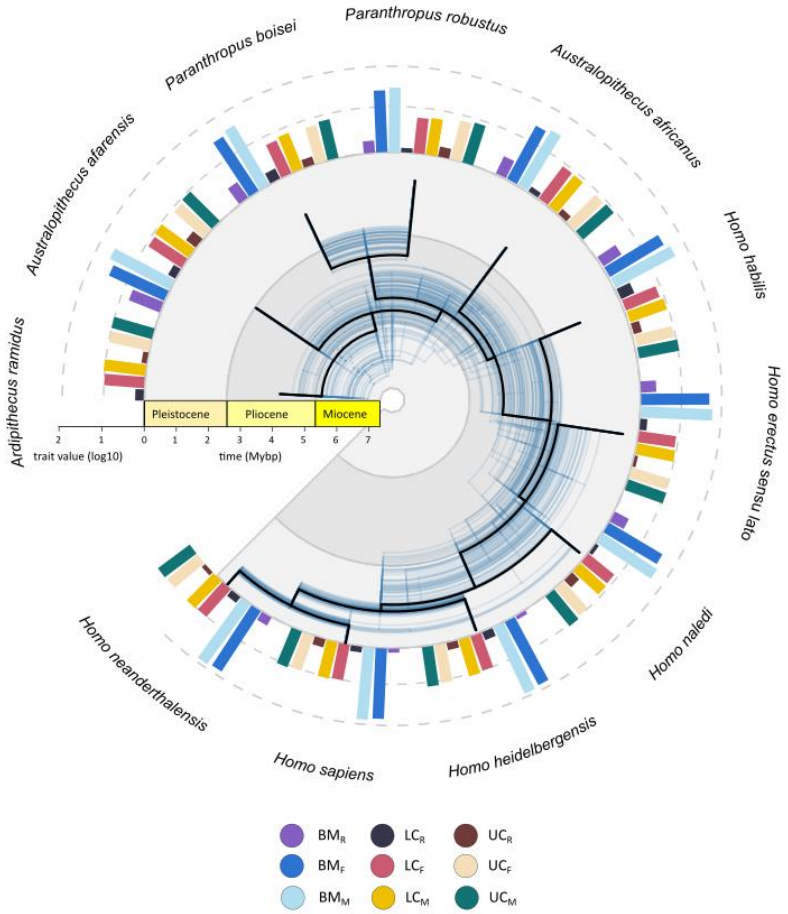

Figure 1. Estimated hominin sexual dimorphism and the sample of phylogenetic trees used for downstream analyses. Coloured bars across phylogenetic tips represent the trait's ratios and sex trait values. The black radial tree represents the maximum clade credibility tree obtained from a Bayesian sample of 1,000 trees. The blue radial trees represent the Bayesian posterior distribution of trees. BM_R: body mass ratio, BM_F: female body mass, BM_M: male body mass, LC_R: lower canine ratio, LC_F: female lower canine size, LC_M: male lower canine size, UC_R: upper canine ratio, UC_F; female upper canine size, UC_M: male lower canine size. The logs of traits ratios were scaled four times to improve visualizations. Plot generated using the *ggtree*[9], *treeio*[10], and *deeptime*[11], R-packages.

Using the estimated ratios, as well as the estimated mean values for each sex, we applied Bayesian phylogenetic comparative analyses in BayesTraits v4[12] to identify the primary sex driving the evolution of sexual dimorphism. This is one of the very unusual situations where we can use ratios to make biological and evolutionary inferences as ratios are attempts to represent real biological features of

species[13,14]. Their correlations with other traits similarly are real rather than just mathematical constructs[13]. We employed the correlation model in BayesTraits which allowed us to estimate the pairwise associations between traits (the evolutionary covariance among traits, r) and the rate of evolution for each trait (the evolutionary variances, σ^2), using a sample of trees to account for phylogenetic uncertainty (Methods). As we estimated these associations simultaneously in a Bayesian phylogenetic context, we can test if covariances and variances are significantly different from each other (Methods).

Evidence for a negative association between BM_R and time would support a reduction in body mass dimorphism over the course of hominin evolution (Figure 2a), as has been inferred from fossil observations[5,15–17]. A negative association between BM_M and time, without corresponding association for BM_F, would support the hypothesis that dimorphism declined owing to a weakening of sexual selection for larger males (Figure 2b)[1–3,5,6]. Conversely, a positive association between BM_F and time, in the absence of a corresponding association for BM_M, would support hypotheses proposing that natural selection for larger females drove the reduction in dimorphism (Figure 2c)[3].

Unlike BM_R, UC_R and LC_R show low levels of dimorphism in hominin remains[5], suggesting that sexual selection for large male canines weakened early in hominin evolution[5,7]. Consequently, we would expect that UC_R and LC_R are decoupled from time (Figure 2d). However, if the reduction of canines were under selection in both sexes, either owing to their increasing use for incisal function[18], because large canines were replaced by handheld tools or other non-canine forms of competition[16,19–21], or owing to mechanical constraints associated with cranial evolution[18,22–25], we should find evidence for time to be negatively association with UC_F, UC_M, LC_F, and LC_M (Figure 1e, f). Furthermore, if natural selection exerted stronger effects on male canines [18], the negative association with time should be more pronounced for UC_M, and LC_M (Figure 1f). Finally, if males experienced greater evolutionary changes in canine size than females [18], we would expect higher evolutionary rates in UC_M and LC_M compared to UC_F and LC_F (Figure 1f).

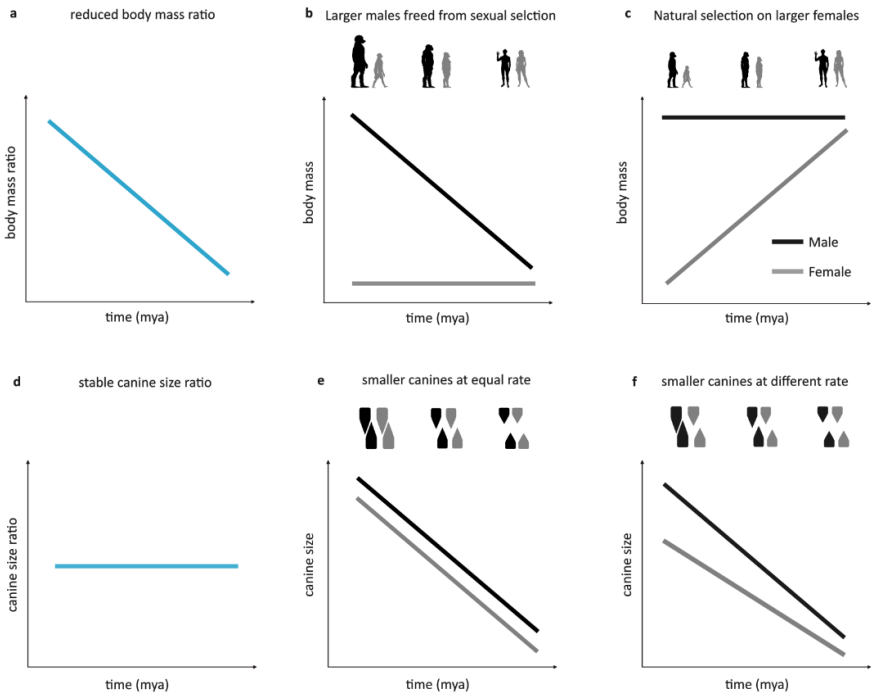

Figure 2. Alternative hypotheses explaining sexual dimorphism evolution in hominins. **a,** the pattern of body mass dimorphism reduction can be explained by either (**b**) the evolution towards smaller males owing to weaking of sexual selection, with females serving as the baseline for comparison; or (**c**) the evolution of larger females owing to natural selection. **d,** the pattern of stable upper and lower canine size dimorphism can be explained by either (**e**) males and females evolving towards smaller canines at similar rates; or by (**d**) males and females evolving towards smaller canines but at higher rates in males.

To test predictions regarding body mass dimorphism evolution, we fitted the phylogenetic correlation model to data on BM_R, BM_F, BM_M, and time, using a sample of hominin trees to account for phylogenetic uncertainty (Methods). From the six pairwise evolutionary associations estimated (Figure 3a), we found that BM_R was negatively associated with time (r_{MEDIAN} $BM_{R,\ TIME}$ = -0.8; $pMCMC_{100}$ > 95; Figure 3a, Figure 4a). BM_R was decoupled from BM_M (r_{MEDIAN} BM_R, BM_M = -0.2; $pMCMC_{92}$ < 95; Figure 3a) but it was negatively associated with BM_F (r_{MEDIAN} BM_R, BM_F = -0.4; $pMCMC_{99.3}$ > 95; Figure 3a). Additionally, BM_M was decoupled from time (r_{MEDIAN} $BM_{M,\ TIME}$ = 0.2; $pMCMC_{67}$ < 95; Figure 3a), and BM_F was positively associated with time (r_{MEDIAN} $BM_{F,\ TIME}$ = 0.5; $pMCMC_{99.7}$ > 95; Figure 3a). Finally, the evolutionary rate of BM_F was statistically higher than the evolutionary rate of BM_M (σ^2 BM_F > σ^2 BM_M; $pMCMC_{98.6}$ > 95; Figure 4d).

These results demonstrates that body mass sexual dimorphism decreased through time, providing robust statistical support for speculations derived from incomplete evidence associated to the hominin fossil record. Additionally, it was the sustained trend towards larger females (Figure 1c), rather than a sustained trend towards smaller males (Figure 1b), that drove the reduction in dimorphism (Figure 1a). The reduction in body mass dimorphism in hominins has usually been attributed to reductions in male body mass which is linked to fundamental changes in social behaviour likely involving a reduction in male–male competition coupled with increased cooperation[1–3,5,6]. However, our findings challenge this interpretation. As such, hypotheses seeking to explain the reduction in body mass dimorphism in human evolution should account for natural selection acting on larger females instead of weakening of sexual selection on larger males. Accordingly, the reduction in body mass dimorphism can be explained by an evolutionary shift towards optimising female reproductive success[3]. This hypothesis is based on the premises that female body mass is subject to additional demands from lactation and pregnancy, which directly influence reproductive success. Larger females are often better equipped to meet the metabolic demands of pregnancy and lactation, leading to increased offspring survival. This is supported by observations that in mammals, including humans [26], larger mothers tend to produce more surviving offspring, partly because they can produce larger, healthier offspring and provide better milk, thus supporting faster growth and higher survival rates. When resources are abundant and reliable, selection tends to favour larger females due to these advantages. In addition, females compete for resources, as males do, and agonistic competition among females for resources has real consequences for reproductive success. Traits that enhance female competition, such as larger body size, may have been subject to selection, thereby contributing to reduced dimorphism.

Regarding lower canine size dimorphism evolution, we evaluated predictions by fitting the phylogenetic correlation model to data on LC_R, LC_F, LC_M, and time, using a sample of hominin trees to account for phylogenetic uncertainty (Methods). From the six pairwise evolutionary associations estimated (Figure 3e), we found that LC_R was decoupled from time (r_{MEDIAN} $LC_{R,\ TIME}$ = -0.2; $pMCMC_{50}$ < 95; Figure 3e; Figure 4b). LC_R was positively associated with LC_M (r_{MEDIAN} LC_R, LC_M = 0.5; $pMCMC_{99.3}$ > 95; Figure 3e) but decoupled from LC_F (r_{MEDIAN} LC_R, LC_F = 0.1; $pMCMC_{88.1}$ < 95; Figure 3e). Additionally, time was negatively associated with LC_M and LC_F (r_{MEDIAN} $LC_{M,\ TIME}$ = -0.6; $pMCMC_{100}$ > 95; r_{MEDIAN} $LC_{F,\ TIME}$ = -0.5; $pMCMC_{100}$ > 95; Figure 3e), without differences regarding the strength of the evolutionary association (r $LC_{F,\ TIME}$ > r $LC_{M,\ TIME}$; $pMCMC_{94.9}$ < 95; Figure 4b) nor between the evolutionary of LC_M and LC_F (σ^2 LC_F > σ^2 LC_M; $pMCMC_{59.1}$ < 95; Figure 4e).

To evaluate prediction associated to upper canine size dimorphism evolution, we fitted the phylogenetic correlation model to data on UC_R, UC_F, UC_M, and time, while accounting for phylogenetic uncertainty (Methods). UC_R was decoupled from time (r_{MEDIAN} $UC_{R,\ TIME}$ = 0.04; $pMCMC_{62.5}$ < 95; Figure 3i; Figure 4c). UC_R was negatively associated with UC_M and UC_F (r_{MEDIAN} UC_R, UC_M = -0.3; $pMCMC_{98.4}$ > 95; r_{MEDIAN} UC_R, UC_F = -0.5; $pMCMC_{99.6}$ > 95; Figure 3i), and the negative association was significantly stronger in females than males (r UC_R, UC_F < r UC_R, UC_M; $pMCMC_{100}$ > 95; Figure 4c). Time was negatively associated with UC_M and UC_F (r_{MEDIAN} $UC_{M,\ TIME}$ = -0.4; $pMCMC_{99}$ > 95; r_{MEDIAN} $UC_{F,\ TIME}$ = -0.3; $pMCMC_{96.8}$ > 95; Figure 3i) without differences in the strength of the negative association (r $UC_{F,\ TIME}$ > r $UC_{M,\ TIME}$; $pMCMC_{63}$ < 95; Figure 4c). However, UC_M evolved at a slower rate than UC_F (σ^2 UC_F > σ^2 UC_M; $pMCMC_{100}$ > 95; Figure 4f).

Our findings showing that both LC_R and UC_R evolved without a sustained trend over time supports the notion that male canine size have been freed from sexual selection through hominin evolutionary history (Figure 1). Additionally, the sustained trend towards lower LC and UC in both sexes, provide support for the idea that natural selection acting on smaller canines either owing to their increasing use for incisal function[18], because large canines were replaced by handheld tools or other non-canine forms of competition[16,19–21], or owing to mechanical constraints associated with cranial evolution[18,22–25], has been prevalent, also supporting the idea that small canines is a defining characteristic of hominins, as it has been long suggested[5,7]. Our results highlighting that the evolutionary rate of UC_F is higher than the UC_M rate, suggest that females UC had greater evolutionary lability and a broader range of variation upon which selection could act. In contrast, UC in males could be subject to stronger stabilising selection, constraining their evolutionary differentiation through time. This could be related to the fact that upper canines are typically more sexually dimorphic than lower canines in primates[1,3], likely owing to their role in male–male competition.

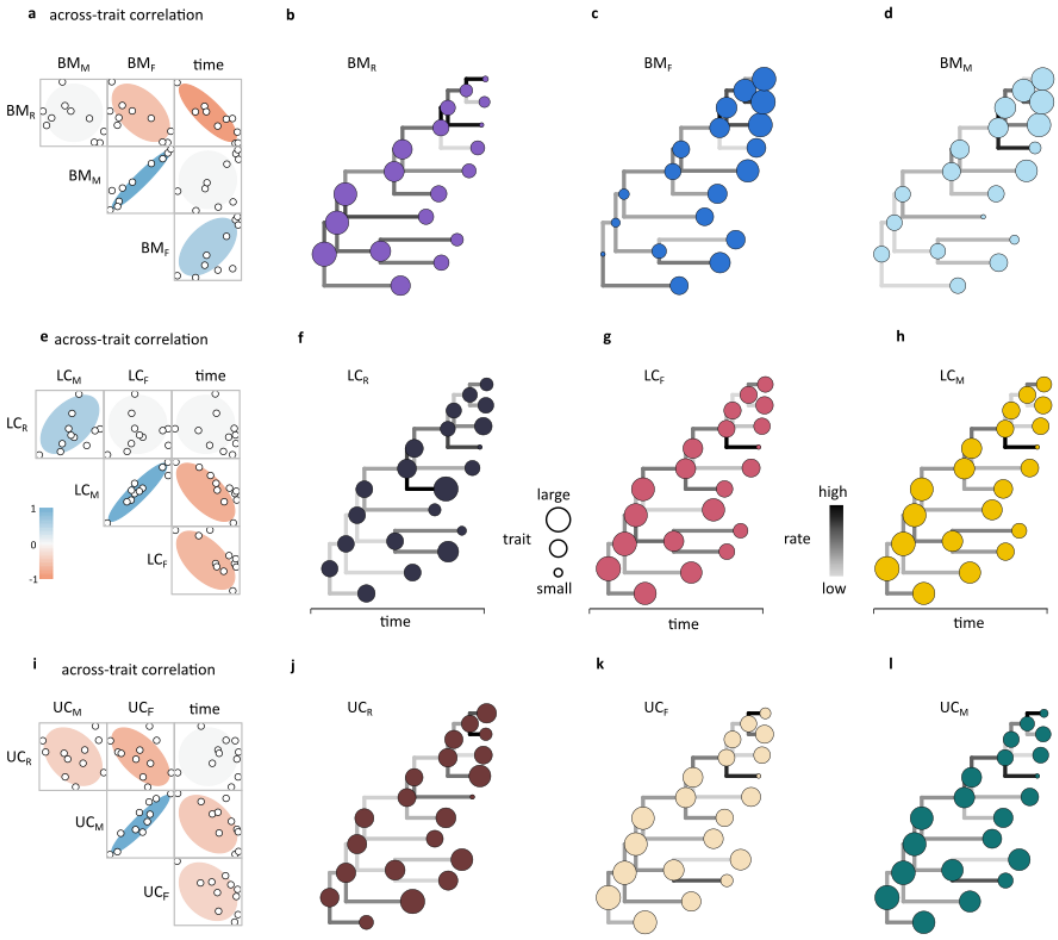

Figure 3. **Across-trait correlations of sexual dimorphism and their evolution through time. a, e, i,** median evolutionary correlations (r) for body mass (**a**), lower canine size (**e**), and upper canine size (**c**). Ellipse shape and colour indicates the strength and direction of the correlations, respectively. Winter white ellipses indicate non-significant correlations. White-filled dots indicate the trait data. **b-d, f-h, j-l,** trait evolution on the hominin's time-calibrated MCC tree. Filled circles at phylogenetic tips indicates the data estimated using the *pdpeak* method while filled circles at internal phylogenetic nodes indicate ancestral states estimated by phylogenetic predictions (see Methods). Grey coloured branches indicate the rate of trait evolution. BM_R: body mass ratio, BM_F: female body mass, BM_M: male body mass, LC_R: lower canine ratio, LC_F: female lower canine size, LC_M: male lower canine size, UC_R: upper canine ratio, UC_F; female upper canine size, UC_M: male lower canine size.

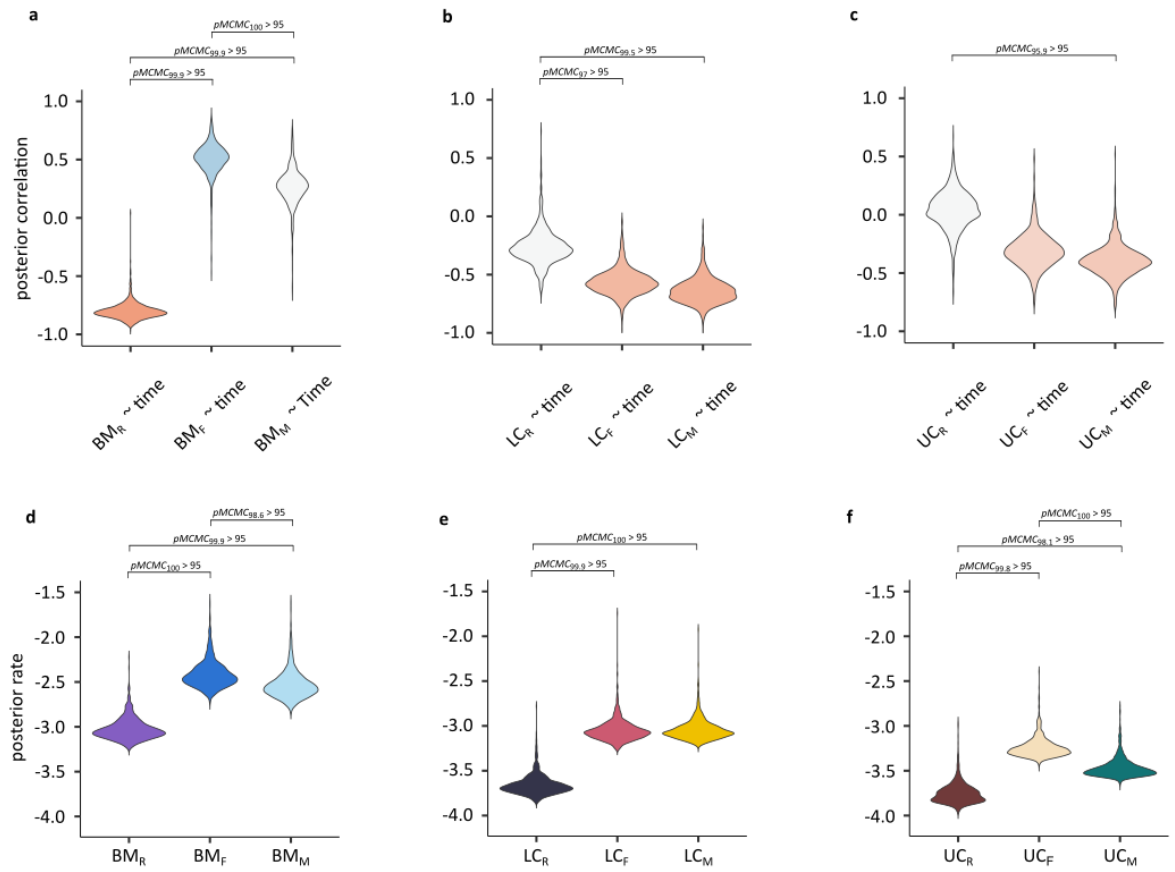

Figure 4. Posterior correlations and rates of sexual dimorphism evolution. a-c, posterior correlation of sexual dimorphism and time. Winter white filled violins indicate non-significant correlations. **d-f,** posterior distribution of evolutionary rates for sexual dimorphism. *pMCMC* values on top of each plot indicate significant differences in pairwise parameter comparisons. BM_R: body mass ratio, BM_F: female body mass, BM_M: male body mass, LC_R: lower canine ratio, LC_F: female lower canine size, LC_M: male lower canine size, UC_R: upper canine ratio, UC_F; female upper canine size, UC_M: male lower canine size.

Taking together, our phylogenetic approach, using dimorphism estimates from fossils, offers a broad perspective on the main driving force behind the evolution of sexual dimorphism in hominin evolution and the potential underlying selective factors. The emerging picture shows a clear evolutionary trend of reduced body mass dimorphism over time, but minimal canine dimorphism since early stages of hominin evolution. This implies that aside from obstetrically related pelvic dimorphism, it is only body mass, and associated skeletal size and robusticity, that remain the primary biologically meaningful hominin dimorphic traits that can be directly observed in the hominin fossil record. Despite debates about the best methods for estimating sexual dimorphism in fossils[8], no approach can fully resolve the challenges posed by the fragmentary and temporally dispersed nature of the fossil record. Size and morphological variation within species, both spatially and through time, introduces unavoidable uncertainty, especially when specimens from different regions and periods are grouped under a single taxon[5]. Still, estimating dimorphism and integrating findings over uncertainty wherever possible remains valuable for informing on aspects of extinct hominin biology related to social structure, mating systems, and behavioural ecology that are otherwise inaccessible. These estimates enrich our understanding of hominin evolution and diversity. When integrated with phylogenetic comparative methods, they provide a rigorous framework for testing evolutionary hypotheses, offering essential insights into crucial processes in human evolution.

Methods

Fossil data

We used the fossil dataset of hominin specimens with body mass from[27]. However, several hominin taxa are known by too few specimens to estimate sexual size dimorphism. Therefore, *Sahelanthropus tchadensis*, *Paranthropus aethiopicus*, *Australopithecus garhi*, and *Kenyanthropus platyops* were removed from our phylogenies, as these species are all represented by too few specimens to provide any indication of whether any size dimorphism was or was not present**.** We also excluded Denisovans from the analysis owing to a lack of sufficient anatomical data. There are too few individuals with adequate anatomical information to establish any level of sexual dimorphism, and all Denisovan teeth with proteomic evidence of sex are from male individuals[28]. This dataset was complemented with canine size data that was gathered from the literature. Canine buccolingual widths were collected from previous publications (Supplementary Table 1), as this measurement is more readily available in fossil individuals as compared to other canine metrics, such as canine height. Right canines were preferred when both antimeres were available for the same specimen. The final dataset comprised body mass (n = 422), upper (n = 324) and lower (n = 324) canine buccolingual widths.

Hominin phylogenetic relationships

A Bayesian sample of 1,000 phylogenetic trees was obtained from a recent study in hominin phylogenetics[27]. These trees were randomly sampled from a posterior distribution of phylogenies obtained using a 'combined evidence' Bayesian phylogenetic reconstruction of hominin species, and based on stratigraphic, molecular, and morphological data. These phylogenetic trees were used in our subsequent phylogenetic analyses.

Estimating sexual dimorphism from fossil data

Determining the degree of sexual dimorphism in a species is typically easy when there are enough physical characteristics that can be used to identify the sex of individuals in a given sample. However, in the case of fossil hominins, estimating sexual dimorphism is much more challenging because fossils are often incomplete, fragmentary, and lack the necessary distinguishing features to provide an accurate sex estimation. Therefore, we applied a recently developed approach, known as pdpeak[4], that overcomes several of the limitations found with previously used approaches. The *pdPeak* method is a Bayesian Mixture Model that simultaneously estimates male-to-female (M/F) ratios and within-sex variance. This dual estimation allows *pdPeak* to provide more accurate and unbiased results, even at lower levels of dimorphism, which brings the unique opportunity to better estimate dimorphism in weakly dimorphic traits like hominins canines[4,7].

The *pdPeak* method uses Bayes theorem to evaluate the likelihood of different parameter combinations (i.e., male mean, female mean, and common within-sex variance), considering the overall shape of the sample distribution. As a result, *pdPeak* offers more reliable estimates of dimorphism across a range of fossil samples, providing a clearer picture of past sexual dimorphism levels in hominins and other species. *pdPeak* was measured for BM, UC and LC by using the script available at https://github.com/sxdm/pdPeak in MATLAB (R2022b; MathWorks). Chains were run for million iterations to achieve convergence and reliable parameter estimates. In addition, mean estimates for female and male body and canine size were calculated using the complete posterior distribution obtained using the *pdPeak* MCMC approach.

As several different dimorphism metrics have been proposed for application to fossils, we assessed the robustness of our results by computing alternative metrics. These dimorphism metrics can be broadly classified into three types based on their computational approach: grouping methods, finite variance-based methods, and finite mixture model methods[8]. Grouping methods involve splitting some or all of the sample into two groups one or more times, then calculating the ratio of the mean of the larger values to the mean of the smaller values. Variance-based methods estimate intraspecific variability in relative size, under the assumption that a major contributor to this variability is the between-sex component. Finite mixture models, meanwhile, also produce ratios of means by assuming the sample derives from

a finite mixture of two underlying distributions (typically female and male size), and then infer the population means of these distributions using information from the observed sample.

Since *pdPeak* corresponds to a finite mixture model, we assessed our results using two additional metrics representatives of the most reliable grouping and variance-based dimorphism methods tested by[8]. We computed the Mean Method Ratio (*MMR*), a grouping method in which a sample is split at the sample mean into a set of larger and a set of smaller measurements. MMR is calculated as the ratio of the mean of the larger measurements to the mean of the smaller ones [29]. As a variance-based method, we simply used the Standard Deviation of Logged Data (*sdlog*). As noted by [30], the standard deviation of log-transformed data serves as a measure of relative size variation and therefore used instead of the coefficient of variation as a variance-based metric. Our comparative results are qualitatively identical regardless of the dimorphism metric used, demonstrating the robustness of our findings.

Finally, we ran all the analyses using two trait-datasets. First, we combined the trait data of *H. erectus*, *H. ergaster*, and Georgian *H. erectus* into a single taxon, *H. erectus* sensu lato. This approach was driven by ongoing debates surrounding the taxonomy of *H. erectus* and its various regional forms. By assigning the *H. erectus* sensu lato data to the phylogenetic tip of *H. ergaster*, we followed the convention of placing the earliest diverging species in the phylogeny at the base, providing a more coherent framework for examining trait evolution across these closely related taxa. Second, we assessed the robustness of our results to the taxonomic combination by using a trait dataset where we considered those three phylogenetic tips as independent taxa. Our results are qualitatively similar regardless of the taxonomic classification used.

Inferring the evolutionary correlations and rates of sexual dimorphism

To simultaneously estimate and compare the evolutionary correlations and rates of evolution of sexual dimorphism, we fitted the correlation model for continuous traits in BayesTraits v4.0 (option 4), using the sample of 1,000 of phylogenetic trees to account for phylogenetic uncertainty. The correlation model simultaneously estimates the posterior distribution of the phylogenetically corrected mean for each trait at the root of the tree (α), the rate of evolution for each trait (σ^2), and the evolutionary correlation (r) between all the pairwise combinations of traits.

We ran three correlation models. First, we fitted a correlation model for BM_R, BM_F, BM_M, and species path length (time). A second correlation model was fitted for LC_R, LC_F, LC_M, and species path length. Finally, a third correlation model was fitted for UC_R, UC_F, UC_M, and species path length. The species path length is the root to tip sum of branch lengths. When branch length is measured in unit of time, the path length represents the amount of time that each species has evolved since the origin of the hominin's most recent common ancestor. Therefore, it allows to study the association between each dimorphic trait and evolutionary time. For example, we can study the association between evolutionary time with body mass dimorphism, while accounting for the relationship between the body mass of each sex and evolutionary time. We additionally obtained the path length from each of the 1,000 phylogenetic trees in the posterior distribution, as well as from the maximum clade credibility (MCC) tree. We obtained the MCC tree using the *maxCladeCred* function of the *phangorn* R-package[31], version 2.12.1.

We ran all the three partial correlation models on the MCC tree and on each of the 1,000 trees in the posterior distribution. We based our interpretation of sexual dimorphism evolution only when the results were statistically significant and consistent in both the MCC tree and in over 95% of the 1,000 trees.

To test for statistical significance of the correlation coefficients we assessed the percentage in which the posterior distribution of the R parameter crossed zero. The correlation coefficient was considered statistically significant if their estimated values crossed zero in over 95% of the iterations within the posterior distribution (i.e., R > 95%). To test for statistically significant differences between pairs-wise comparison of correlation coefficients (e.g., $r_{Trait1,2}$ vs $r_{Trait3,4}$), and pair-wise comparisons of trait evolutionary rates (e.g., σ^2_{Trait1} vs σ^2_{Trait2}), we assessed the percentage of iterations in which one parameter was higher/lower than the other parameter. Parameters were considered statistically different

if their estimated values were consistently higher or lower in over 95% of the iterations within the posterior distribution. Finally, we ran each chain for 21 million iterations, discarding the first 11 million iteration as burn-in, and sampling every 10,000 iterations.

Phylogenetic prediction of sexual dimorphism. To get a visual representation of sexual dimorphism evolution in the hominin phylogenetic tree, we conducted a phylogenetic predictive approach to estimate unknow values of dimorphism at phylogenetic nodes. Phylogenetic prediction refers to estimating unknown species (tip) values based on the know values of other species, leveraging the structure of the phylogenetic tree and assumption of an evolutionary mode[32]. We followed the approach in reference [33] where ancestral states are estimated by placing zero branch-length "false tips" at each internal node. We based our phylogenetic prediction on the MCC tree of hominins. We estimated the maximum likelihood of unknown values of dimorphism at each "false tip" based on the "known" values of time at each phylogenetic node and the known association of dimorphism and time across tips. We estimated values of LCR and UCR using ancestral state reconstruction based on Brownian motion (without considering their association with time as supported by our correlation analyses). We estimated ancestral states for these ratios using the *ace* function of *ape* R-package[34].

Acknowledgments

We are grateful to Joanna Baker, Jacob Gardner, Suzy White, Carolynne Roberts, Olivia Price, Kerry Stewart, and George Butler, for helpful discussion. This work was funded by a Leverhulme Trust Research Leadership Award to CV (RL-2019-012).

References

1. Plavcan, J. M. Sexual dimorphism in primate evolution. *Am J Phys Anthropol* **116**, 25 (2001).
2. Plavcan, J. M. Inferring social behavior from sexual dimorphism in the fossil record. *J Hum Evol* **39**, 327–344 (2000).
3. Plavcan, J. M. Understanding dimorphism as a function of changes in male and female traits. *Evolutionary Anthropology: Issues, News, and Reviews* **20**, 143–155 (2011).
4. Sasaki, T. *et al.* Estimating sexual size dimorphism in fossil species from posterior probability densities. *Proceedings of the National Academy of Sciences* **118**, (2021).
5. Plavcan, J. M. Sexual Dimorphism in Hominin Ancestors. in *The International Encyclopedia of Anthropology* 1–6 (Wiley, 2018). doi:10.1002/9781118924396.wbiea2195.
6. Lindenfors, P. & Tullberg, B. S. Phylogenetic analyses of primate size evolution: the consequences of sexual selection. *Biological Journal of the Linnean Society* **64**, 413–447 (1998).
7. Suwa, G. *et al.* Canine sexual dimorphism in Ardipithecus ramidus was nearly human-like. *Proceedings of the National Academy of Sciences* **118**, (2021).
8. Gordon, A. D. Interpreting statistical significance in hominin dimorphism: Power and Type I error rates for resampling tests of univariate and missing-data multivariate size dimorphism estimation methods in the fossil record. *J Hum Evol* **199**, 103630 (2025).
9. Yu, G., Smith, D. K., Zhu, H., Guan, Y. & Lam, T. T. GGTREE: an R package for visualization and annotation of phylogenetic trees with their covariates and other associated data. *Methods Ecol Evol* **8**, 28–36 (2017).
10. Wang, L.-G. *et al.* Treeio: An R Package for Phylogenetic Tree Input and Output with Richly Annotated and Associated Data. *Mol Biol Evol* **37**, 599–603 (2020).
11. Gearty, W. deeptime: an R package that facilitates highly customizable and reproducible visualizations of data over geological time intervals. Preprint at https://doi.org/10.31223/X5841N (2025).
12. Pagel, M., Meade, A. & Barker, D. Bayesian estimation of ancestral character states on phylogenies. *Syst Biol* **53**, 673–684 (2004).
13. Smith, R. J. Statistics of sexual size dimorphism. *J Hum Evol* **36**, 423–458 (1999).
14. Liker, A. *et al.* Evolution of large males is associated with female-skewed adult sex ratios in amniotes. *Evolution (N Y)* **75**, 1636–1649 (2021).

15. Gordon, A. D., Green, D. J. & Richmond, B. G. Strong postcranial size dimorphism in *Australopithecus afarensis* : Results from two new resampling methods for multivariate data sets with missing data. *Am J Phys Anthropol* **135**, 311–328 (2008).
16. McHenry, H. M. Body size and proportions in early hominids. *Am J Phys Anthropol* **87**, 407–431 (1992).
17. Larsen, C. S. Equality for the sexes in human evolution? Early hominid sexual dimorphism and implications for mating systems and social behavior. *Proceedings of the National Academy of Sciences* **100**, 9103–9104 (2003).
18. Greenfield, L. O. Origin of the human canine: A new solution to an old enigma. *Am J Phys Anthropol* **35**, 153–185 (1992).
19. Darwin, C. *The Descent of Man, and Selection in Relation to Sex, Vol 1.* (John Murray, London, 1871). doi:10.1037/12293-000.
20. McHenry, H. M. Behavioral ecological implications of early hominid body size. *J Hum Evol* **27**, 77–87 (1994).
21. McHenry, H. M. Sexual Dimorphism in Fossil Hominids and its Socioecological Implications. in *The Archaeology of Human Ancestry* (eds. Shennan, S. & Steele, J.) 91–109 (Routledge and Kegan Paul, London, 1995).
22. Leutenegger, W. & Shell, B. Variability and sexual dimorphism in canine size of Australopithecus and extant hominoids. *J Hum Evol* **16**, 359–367 (1987).
23. Greenfield, L. O. Unicausal theories of human canine evolution: are they sufficient? *Z Morphol Anthropol* **78**, 155–68 (1990).
24. Greenfield, L. O. Canine reduction in early man: A critique of three mechanical models. *Hum Evol* **5**, 213–226 (1990).
25. Greenfield, L. O. Canine "honing" in *Australopithecus afarensis*. *Am J Phys Anthropol* **82**, 135–143 (1990).
26. Ralls, K. Mammals in Which Females are Larger Than Males. *Q Rev Biol* **51**, 245–276 (1976).
27. Püschel, T. A., Nicholson, S. L., Baker, J., Barton, R. A. & Venditti, C. Hominin brain size increase has emerged from within-species encephalization. *Proceedings of the National Academy of Sciences* **121**, (2024).
28. Tsutaya, T. *et al.* A male Denisovan mandible from Pleistocene Taiwan. *Science (1979)* **388**, 176–180 (2025).
29. Godfrey, L. R., Lyon, S. K. & Sutherland, M. R. Sexual dimorphism in large-bodied primates: The case of the subfossil lemurs. *Am J Phys Anthropol* **90**, 315–334 (1993).
30. Plavcan, J. M. & Cope, D. A. Metric variation and species recognition in the fossil record. *Evolutionary Anthropology: Issues, News, and Reviews* **10**, 204–222 (2001).
31. Schliep, K. P. phangorn: phylogenetic analysis in R. *Bioinformatics* **27**, 592–593 (2011).
32. Organ, C. L., Shedlock, A. M., Meade, A., Pagel, M. & Edwards, S. V. Origin of avian genome size and structure in non-avian dinosaurs. *Nature* **446**, 180–184 (2007).
33. Baker, J., Meade, A., Pagel, M. & Venditti, C. Adaptive evolution toward larger size in mammals. *Proc Natl Acad Sci U S A* **112**, 5093–5098 (2015).
34. Paradis, E. & Schliep, K. ape 5.0: an environment for modern phylogenetics and evolutionary analyses in R. *Bioinformatics* **35**, 526–528 (2019).